

“Salt crystallization in pores: quantification and estimation of damage”

Matthieu Angeli¹, Jean-Philippe Bigas¹, David Benavente², Beatriz Menéndez¹, Ronan Hébert¹ and Christian David¹

¹ Université de Cergy-Pontoise
Département de Sciences de la Terre et Environnement
5 mail Gay-Lussac, Neuville-sur-Oise
95031 Cergy-Pontoise CEDEX
France

² Universidad de Alicante
Departamento de Ciencias de la Tierra y del Medio Ambiente
Laboratorio de Petrología Aplicada
Apartado 99
03080 Alicante
España

Published in a special issue on salt decay for Environmental Geology: Angeli M., Bigas JP, Benavente D, Menéndez B, Hébert R. and David C. 2007 – Salt crystallization in pores: quantification and estimation of damage – Environmental geology, 52:205-214

Abstract

The objective of this study is to understand and predict the alteration of any rock by crystallization of salts. Samples of different rocks have been tested thanks to the EN 12370 standard test. Two parameters are proposed to evaluate the alteration of a rock during these tests. The alteration index AI represents the cycles in which the first damages occur. The alteration velocity AV is the alteration rate at the end of the experiment, when the decay has become regular. These parameters can be estimated with the help of a microstructural study of the rocks. The intrinsic parameters of the stones that are the most relevant for this estimation are capillary coefficient, evaporation coefficient, tensile strength and P-waves velocity. An evaluation of the alteration pattern is also proposed depending on the eventual heterogeneities and anisotropies of the rocks. The influence of the dimension and shape of the samples is also discussed.

Résumé

L'objectif de cette étude est de comprendre et prévoir l'altération d'une roche par la cristallisation de sels. Des échantillons de différentes roches ont été testées selon la norme européenne EN 12370. Deux paramètres sont proposés pour évaluer l'altération des échantillons pendant ces tests. L'indice d'altération AI représente le numéro du cycle où les premiers dégâts apparaissent. La vitesse d'altération AV est le taux d'altération à la fin de l'expérience, quand celle-ci est devenue régulière. Ces paramètres peuvent être estimés avec l'aide d'une étude microstructurale des roches. Les paramètres intrinsèques qui sont les plus pertinents pour cette estimation sont le coefficient capillaire, le coefficient d'évaporation, la résistance en traction et la vitesse des ondes P. Une évaluation de la forme générale des altérations est aussi proposée en fonction des éventuelles anisotropies et hétérogénéités. L'influence des formes et dimensions des échantillons sur l'altération est aussi discutée.

Introduction

Salts, and particularly sodium sulphate, are known to be among the most destructive agents in porous stones, concrete or brick weathering. Their study is thus very important to fully understand their crystallization process in porous networks and, in the future, to find a way to prevent or limit their damage to porous materials. Recent studies attribute the decay to the salt crystallization pressure of mirabilite ($\text{Na}_2\text{SO}_4 \cdot 10\text{H}_2\text{O}$), rather than thenardite (Na_2SO_4) (Rodriguez-Navarro & Doehne 1999, Scherer 1999, Flatt 2002, Benavente et al. 2004a, Steiger 2005). This damage depends on the quantity of salt in the stone as well as the characteristics of the porous network (a review can be found in Steiger, 2005).

This study aims to evaluate building stone behaviour during accelerated ageing, and to understand how the porous network is affected. Then weathering will be quantified by few intrinsic parameters and evaluated thanks to a microstructural study. A review about estimation of damage can be found in Benavente et al. (2004b). Most of existing estimators evaluate weathering with only one parameter. This study proposes two parameters, the alteration index (AI) and the alteration velocity (AV), to quantify weathering, and a method to preview how these damages will be organised in the stone. The influence of the shape and dimensions of the samples is also discussed.

1. Materials and Methods

1.1. Materials

Nine stones from different lithologies have been used in this study: four limestones and five sandstones. The four limestones come from the Parisian Basin. Three of them are of lutetian age: the “roche fine” (FL), the “roche franche” (RL) and the “liais” (LL). These three limestones have high porosity compared to the other stones in this study (respectively 37.2, 18.5 and 14.4%). FL is a detritic limestone made of calcite (90%) and quartz (10%). Its tensile strength is very low (1.5 MPa). RL and LL are two boundstones composed by more than 90% of calcite, with traces of iron oxides. They also contain some macrofossils (bivalves, gasteropods) responsible of an heterogeneous aspect. The other limestone is of bartonian age: the “Pierre de Souppes” (SL), a variety of the “Calcaire de Chateau-Landon”. It is just made of calcite. Its porosity is low (4.2%) and its tensile strength high (5.2 MPa).

Two sandstones are Fontainebleau sandstones (Oligocene). These two varieties are called hard (HF) and soft (SF). They are composed of more than 99% of quartz. Their porosity are low (respectively 4.1 and 5.5%). The main difference between the two is their tensile strength: very high for HF (5.2MPa) and very low for SF (1.5 MPa). The three others sandstones are three layered sandstones: one from China: the white sandstone (CS); and two from India: the green sandstone (VS) and the brown sandstone (MS). The white sandstone is composed of more than 99% of quartz. The two others are also composed mostly of quartz, but contain some clay which give the general colour of the rock. All three sandstones present a very high tensile strength (6.1, 15.0 and 16.0 MPa) and low porosity (2.6, 4.5 and 4.7%). Complete hydromechanic properties of these nine sedimentary rocks are given in table 1.

The capillary coefficient C is the sorptivity expressed in $g/(m^2 \cdot s^{1/2})$. The evaporation coefficient E is also expressed in $g/(m^2 \cdot s^{1/2})$, and corresponds to the slope of the curve representing the weight loss as a function of the square root of time. This parameter is related to the diffusive part of evaporation (second stage), during which the external conditions (temperature, relative humidity or wind) have no influence (Hammecker 1993).

1.2. *Methods*

Two experiments have been performed, according to the EN 12370 standard about stone resistance to crystallization of salts in pores. They differ in the size and shape of the samples and in the number of cycles. They are composed of cycles which last 24h:

- 2 hours of immersion in a saturated solution with respect to sodium sulfate (14 wt. %);
- 15 hours of drying at 105°C in order to prevent mirabilite crystallization during drying of the samples (Fig. 1);
- 7 hours of cooling at room temperature (20-25°C, 30-40% relative humidity RH). The samples were weighed after 2 hours during this stage.

The first test concerns $4 \times 4 \times 4 \text{ cm}^3$ cubes with two samples per type of stone (18 cubes in total). The test has been run for 30 cycles. In the second test, cylinders of 2.5 cm diameter and 4.5 cm height were used. Two samples of each stone were used for all stones except FL (5 samples), SF (4 samples) and WS (1 sample), that is 22 cylinders. Most of the samples suffered 15 cycles except one sample of FL and one of RL (11 cycles).

	porosity	absorption	bulk density	evaporation coef.	capillary coef.	mean pore radius	P wave velocity	tensile strength
	%	%	g/cm ³	g/m ² /s ^{1/2}	g/m ² /s ^{1/2}	μm	m/s	MPa
liais (St Maximin) LL	14,4	58,2	2,3	26,7	32,25	0,444	4879	4,2
roche franche (St Maximin) RL	18,5	59,7	2,2	40,7	37,55	4,710	4645	3,0
roche fine (St Maximin) FL	37,2	75,9	1,7	66,9	1106,1	12,004	2898	1,5
pierre de Souppes SL	4,2	55,0	2,57	8,0	1,47	0,082	6249	5,2
hard Fontainebleau HF	4,1	29,0	2,54	15,4	6,39	2,866	3903	5,2
soft Fontainebleau SF	5,5	48,2	2,5	12,6	40,12	3,761	1514	1,5
white CS	2,6	94,2	2,6	6,4	5,45	0,310	3329	6,1
green VS	4,5	88,3	2,54	12,3	5,81	0,047	4598	15,0
brown MS	4,7	81,5	2,53	10,5	3,86	0,034	5115	16,0

Table 1. Hydromechanic properties of the studied stones

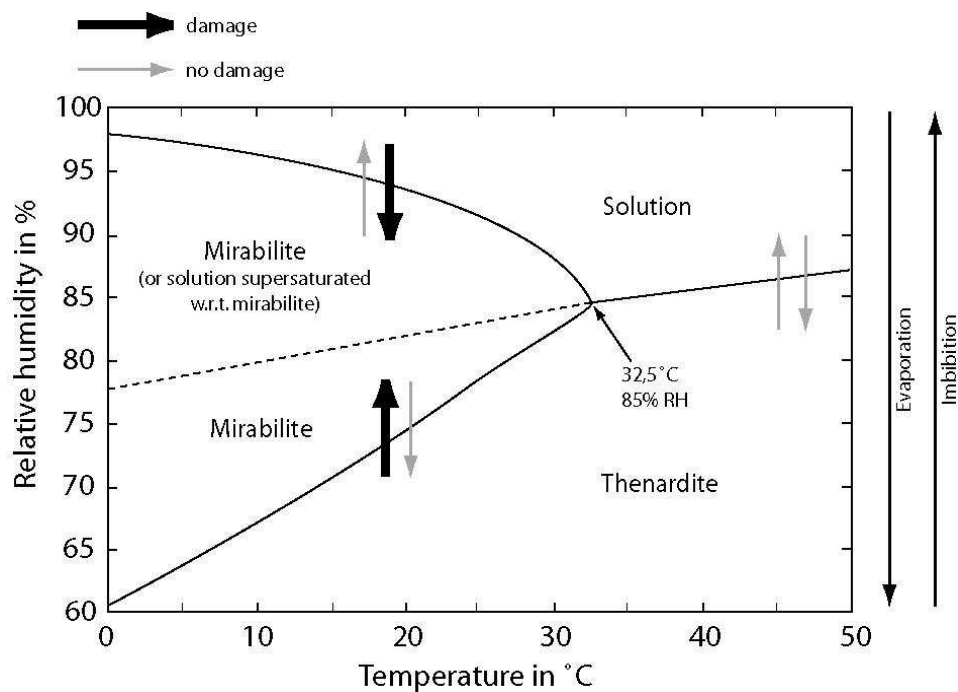


Figure 1. Phase diagram of mirabilite (after Flatt 2002, data from Kracek 1928)

2. Results

2.1. Quantification of alteration

2.1.1. Representation of results

For each sample, results are plotted in diagrams showing normalised weight vs number of cycles. Three representative examples of those graphs are presented on figures 2a, 2b and 2c. All the samples show the same evolution as a function of time. It can be described in two or three stages that are:

- stage I: weight increase due to salt supply;
- stage II (sometimes inexistent, starts after the first visual damage): weight variation depending on a competition between salt supply and stone damage. It can be either a weight increase or decrease;
- stage III: weight decrease because salt uptake becomes negligible compared to stone damage.

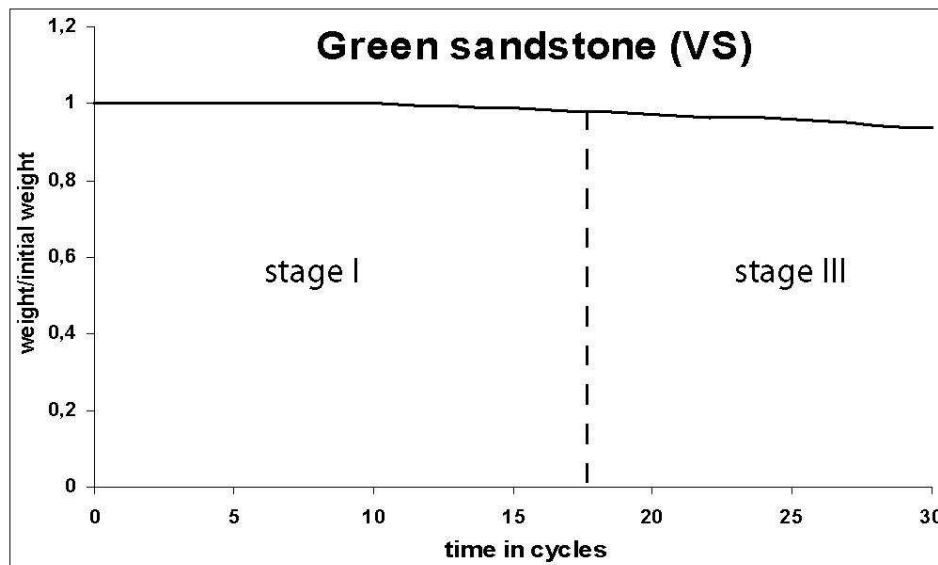


Figure 2a. Normalized weight evolution during the 30 cycles (first test) of a VS sample.

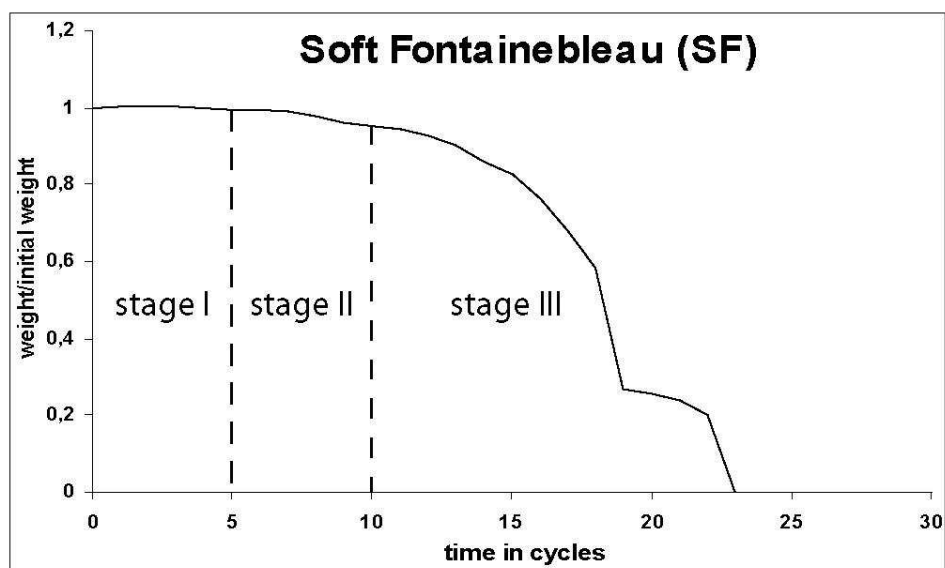


Figure 2b. Normalized weight evolution during the 30 cycles (first test) of a SF sample.

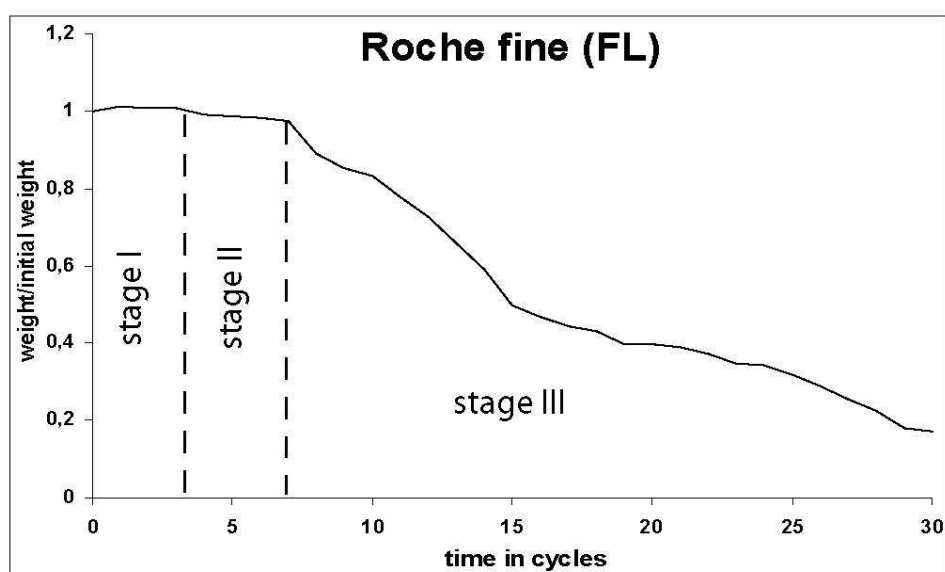


Figure 2c. Normalized weight evolution during the 30 cycles (first test) of a FL sample.

2.1.2. The Alteration Index

The alteration index (AI; Angeli et al. 2006) is defined as the number of the cycle during which the first visible damage occurs (Table 2). This damage, which is firstly esthetical, may imply a change of physical properties, and happens the first time the crystallization pressure is high enough to alter the stone. AI depends only on water circulation possibility, and on mechanical strength (the tensile strength, which evaluates the cohesion

between the grains). According to AI, it is possible to classify the nine studied rocks into three categories:

- high AI (19 and more in experiment 1, 10 and more in experiment 2): SL, HF, MS;
- medium AI (10 to 18 in experiment 1, 5 to 9 in experiment 2): LL, RL, CS, VS;
- low AI (up to 8 in experiment 1, up to 5 in experiment 2): FL, SF.

AI does not represent exactly the stone resistance to salt crystallization, since some stone can present visual damage rapidly and alter slowly afterwards (e. g. VS with relatively low AI compared to its actual durability). On the opposite, some stones can seem rather resistant at first, have no visual damage during few cycles, and then totally break down in 3 or 4 cycles (e. g. CS with relatively high AI compared to its durability). This observation leads to the introduction of the concept of alteration velocity (AV).

	Experience 1 (cubes)			Experience 2 (cylinders)		
		Alteration Index	Alteration Velocity		Alteration Index	Alteration Velocity
liais LL	L7	19	1,33	L3	8	0,19
	L8	13	1,93	L4	9	0,25
roche franche RL	R7	17	3,78	R3	7	4,32
	R8	11	3,62	R4	7	2,80
roche fine FL	F7	3	1,81	F1	3	8,25
	F8	3	2,40	F3	3	9,52
				F4	3	8,58
				F5	4	8,14
				F6	3	9,18
pierre de Souppes SL	S1	19	0,07	S2	13	0,10
	S2	20	0,13	S3	12	0,05
grès dur HF	D1	19	0,06	D2	12	0,46
	D2	19	0,10	D3	10	0,12
grès tendre SF	T1	6	4,02	T1	2	43,90
	T2	5	10,93	T4	2	29,71
				T5	2	32,77
				T6	3	31,63
white sandstone CS	C1	15	5,94	C3	9	5,81
	C2	13	8,10			
green sandstone VS	V1	16	0,30	V2	9	0,68
	V2	17	0,34	V3	9	0,59
brown sandstone MS	M1	23	0,16	M1	12	0,17
	M2	23	0,16	M3	11	0,30

Table 2. Alteration index and alteration velocity for the tested samples

2.1.3. *The Alteration Velocity*

The alteration velocity (AV) is introduced to evaluate the process of weathering in longer term than AI. Mostly, in usual characterization of weathering, only the dry weight loss of samples at a certain stage is used (EN 12370). But the results can be very different if the experiment is stopped after 10 or 20 cycles. AV is used to evaluate the long term behaviour of the stone independently of the number of cycles. It is the final value of the derivative of the function representing the normalised weight as a function of the number of cycles (Table 2). The nine stones can also be classified by their AV:

- low AV (up to 1 %weight/cycle for both experiments): SL, HF, VS, MS;
- medium AV (1 to 5 in experiment 1, 1 to 10 in experiment 2): LL, RL, FL;
- high AV (5 and more in experiment 1, 10 and more in experiment 2): SF, CS.

It is important to notice that the classification is different for AI and AV indicating that these two parameters are independent from each other. It suggests that these two parameters must be used together in order to evaluate more accurately the ageing of the stone.

2.2. *Alteration pattern*

A careful observation of samples through weathering cycles allow to distinguish two different categories of alteration patterns. Figure 3 shows three examples of these alteration patterns. The size of the pictures is 4.5cmx4.5cm, the original size of the samples being 4cmx4cm.

2.2.1. *Homo/Heterogeneity*

It is possible to evaluate the regularity of the weathering of a set of samples from the same type of stone. Some stones present a regular weathering, starting with the progressive smoothing of corners and edges. This type of weathering is regarded as homogeneous, which means it is regular for one sample and approximately the same from a sample to another. Figure 3a gives a good example of this alteration for the FL. The stones which present a homogeneous behaviour are FL, SL and HF.

On the other hand, some stones present various alteration behaviours from one sample to another from the same type of rock, even from one zone to another in a single sample. This is due to pre-existent heterogeneities in the rock. These heterogeneities act as local

weaknesses, and thus differential weathering can occur. These weaknesses can be obvious (e. g. fossils in RL or LL) or hidden (e. g. very competent zone in SF, Fig. 3b). They can either consolidate or weaken the sample. For instance, a fossil creates a weak zone and when this zone breaks, the entire fossil can fall at once, even if the fossil itself is not altered. The stone with a heterogeneous decay are LL, RL and SF.

2.2.2. *Anisotropy*

The second type of alteration pattern concerns anisotropy. It means that alteration has a favourite direction for a stone (Fig. 3c). Anisotropy is an intrinsic property of the material and if it exists, it controls the anisotropy of decay. Four different origins can be identified: the grains (mineral composition due to sedimentation, shapes and orientation), the pores (shape, orientation), the joints and the fractures. This predisposition will influence the decay in several ways: for example, layers that contain hygroscopic clays can cause damage during imbibition, less competent layers can be damaged easier by salt crystallization pressure, cracks can act as a localisation of crystallization and thus of damage... The stones from this study which present anisotropy in the decay are CS, VS and MS.



Figure 3a. Sample of FL after 15 cycles:
homogeneous behaviour.



Figure 3b. Sample of SF after 15 cycles:
heterogeneous behaviour.

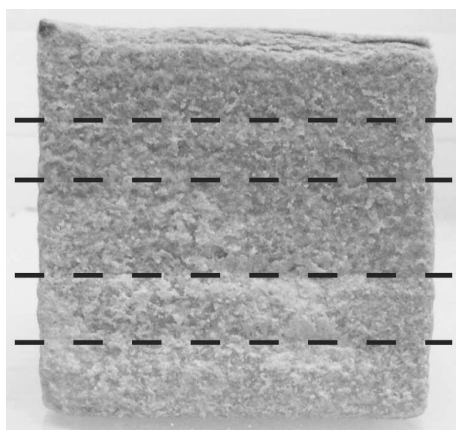


Figure 3c. Sample of VS after 15 cycles: anisotropic behaviour.

3. Discussion

3.1. *The stages of accelerated ageing*

The duration and importance of the three stages of accelerated ageing (I, II, III) depend on the microstructure of the stone. During stage I, weight increase depends mainly on the characteristics of the porous network (porosity, pore size distribution...). The process of crystallization in pores starts during the evaporation. At first, all the pores that can be reached by capillary rise are filled with the brine. During the first stage of evaporation, the capillary phase, the solution and the ions it contains are driven out of the porous network. This means that all the salt here only crystallizes as efflorescences on the surface of the samples. The most important stage of evaporation starts at this moment: when the continuity of water is broken in the sample, the diffusion stage of evaporation starts (Fig. 4). The water starts to circulate as vapour in the porous network, thus allowing salts to crystallize in pores. Stage I stops as soon as enough salt has crystallized in pores to allow further supersaturation and cause damage to the sample (Flatt 2002).

Then there are two possibilities: the first visual damage is either before the loss of weight or after. When the first visual damage occurs before the loss of weight, there is still room in the sample for salt to crystallize, and the loss of material is inferior to its salt uptake. The weight variation is then a competition of these two processes, and there is a stage II. When the loss of weight occurs first, it means that most of the room where salt can crystallize has been filled up. The damage starts when the stresses created by the crystallization pressure

and transmitted through the supersaturated solution is higher than the stone's tensile strength, and in this case there is no stage II.

Phase III starts when the relationship between normalized weight and the number of cycles starts to become approximately linear (Figs. 2a, 2c), i. e. when the salt uptake starts to be negligible compared to material loss. More precisely, it is linear for homogeneous stones. For the heterogeneous stones, the curve shows several steps, which are each approximately linear, but separated by sudden drops (Fig. 2b). For instance, for RL or LL, these drops can be caused by the loss of an entire fossil.

3.2. *Estimators*

3.2.1. *Alteration Index*

In order to estimate the alteration index, a decomposition of the process of accelerated salt weathering has been proposed. This decomposition is based on the existing works about the phase diagram of sodium sulphate (Flatt 2002) and on the drying kinetics presented in figure 8:

- imbibition of saline solution: pores are invaded by the brine;
- as relative humidity (RH) grows, thenardite hydrates into mirabilite by dissolution and reprecipitation (Rodriguez-Navarro et al. 2000) if temperature is below 32.5°C;
- with even higher RH, mirabilite is dissolved in the brine. Here stops the imbibition phase.
- evaporation starts with capillary evaporation and development of efflorescences;
- diffusive evaporation and crystallization of thenardite in the pores.

The crucial phase of this scheme is the crystallization of mirabilite in the pores after the dissolution of thenardite, when the temperature is below 32.5°C (Rodriguez-Navarro and Doehne 1999): this is the part of the cycle when the damages occur. The first damage will anyway appear on the weakest part of the sample. The only characteristics that matter are the hydric properties (capillary C and evaporation E coefficients both in $\text{g}/(\text{m}^2 \cdot \text{s}^{1/2})$) and the mechanical strength of the weakest part of the rock (tensile strength σ_T in MPa). This corresponds also to the parameters used in the estimation of the crystallization pressure for most models (Benavente et al. 2004b, Scherer 2004).

It is also important to recall that this study is only about sodium sulphate, and thus the estimator is only valid for damages induced by sodium sulphate crystallization. Figure 5a and 5b represent the estimator of AI (1) as a function of AI for the two experiments.

$$AI_{estim} = \ln\left(\frac{100.C}{E.\sqrt{\sigma_T}}\right) \quad (1)$$

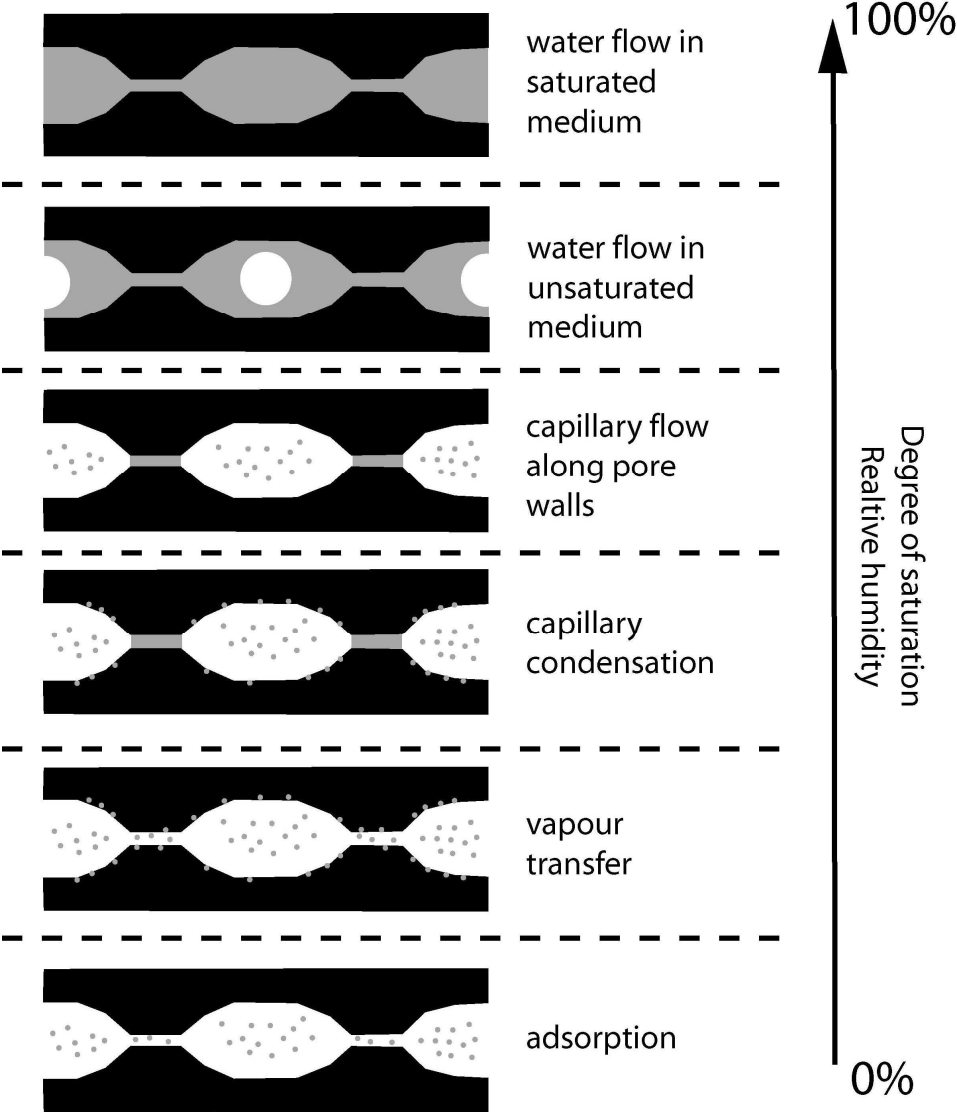


Figure 4. Stages in the wetting of a porous system (Beck et al. 2003, after Rose 1963).

3.2.2. Alteration Velocity

During stage III, the pores are considered to be always filled with salt and the supersaturation with respect to mirabilite reached at every cycle. The salts will crystallize and cause damages in the cracks and pores. Thus the more pre-existing cracks and pores in the rock, the more damage. And also the more cracks and pores in a rock, the lower the P-waves velocity (V_p).

On the other hand, these damages will be more important if the joints between the grains are weak, since in this case the cohesion of the stone is lower. When the grains are weakly bonded, the loss of energy at the interfaces is higher and thus V_p decreases.

These two features have the same influence on V_p . This means that V_p can estimate the long term behaviour of a rock. Since this long term behaviour is given by AV, V_p can be considered as a good trend for AV. However, the low values of the coefficient of determination of the linear regression (R^2) given on figures 6a and 6b show that it can not still be considered as a good estimator.

A part of this error comes from the fact that the velocity of the P-waves is slightly different in quartz (6050m/s) and in calcite (6600m/s). Another part comes also from the fact that one of the two cubes of SF turned out to be much more competent than the others, as competent as HF. If this value is withdrawn from the experimental values, R^2 rises up to 0.61 (instead of 0.45). The presence of clays can also be very damaging to a stone while not having a strong influence on the estimator, and by this could make this estimation incorrect.

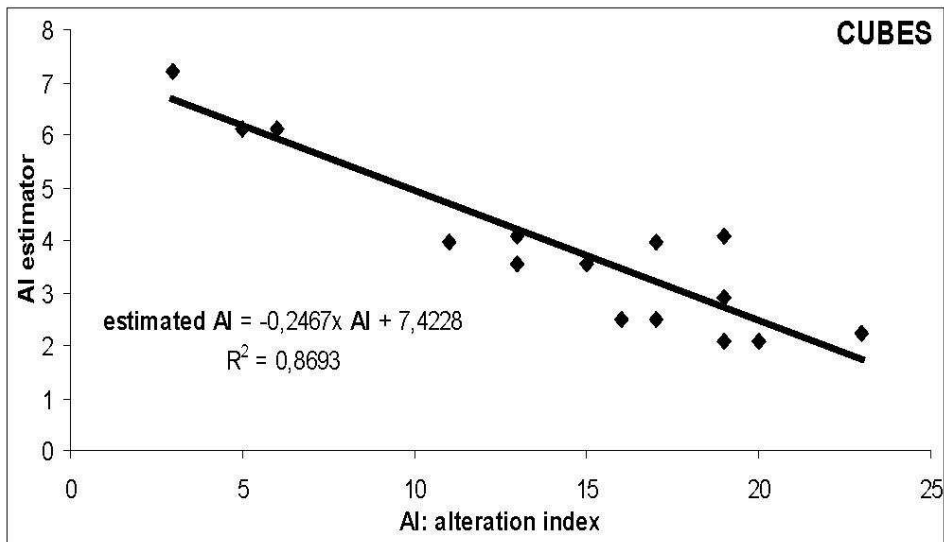


Figure 5a. Estimation of the AI for the first experiment.

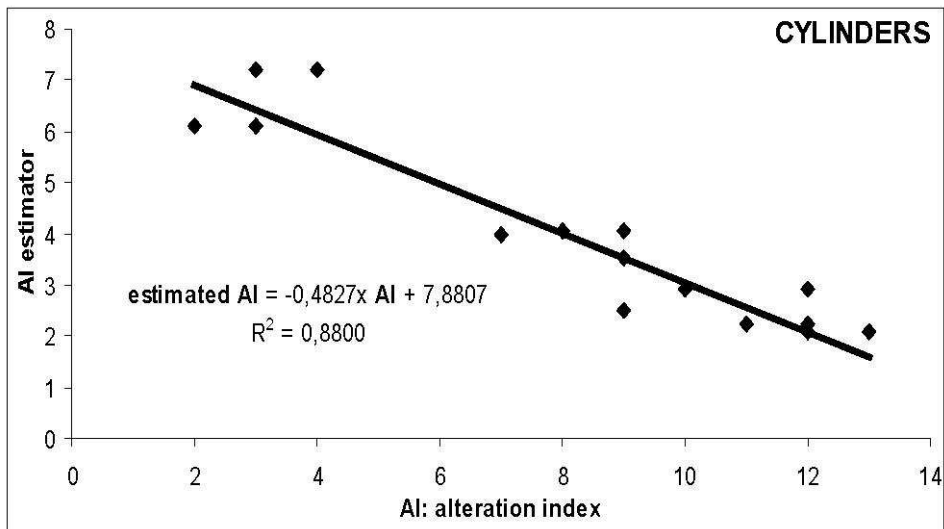


Figure 5b. Estimation of the AI for the second experiment.

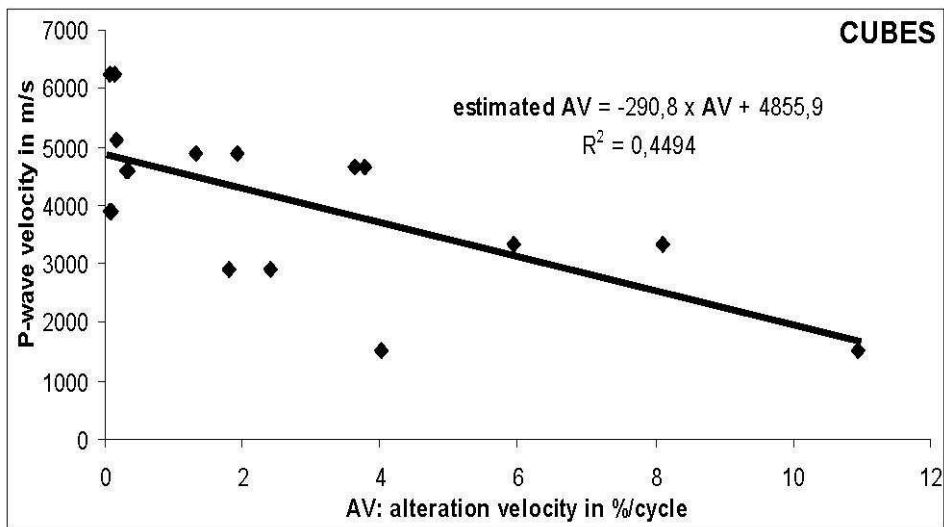


Figure 6a. Estimation of the AV for the first experiment.

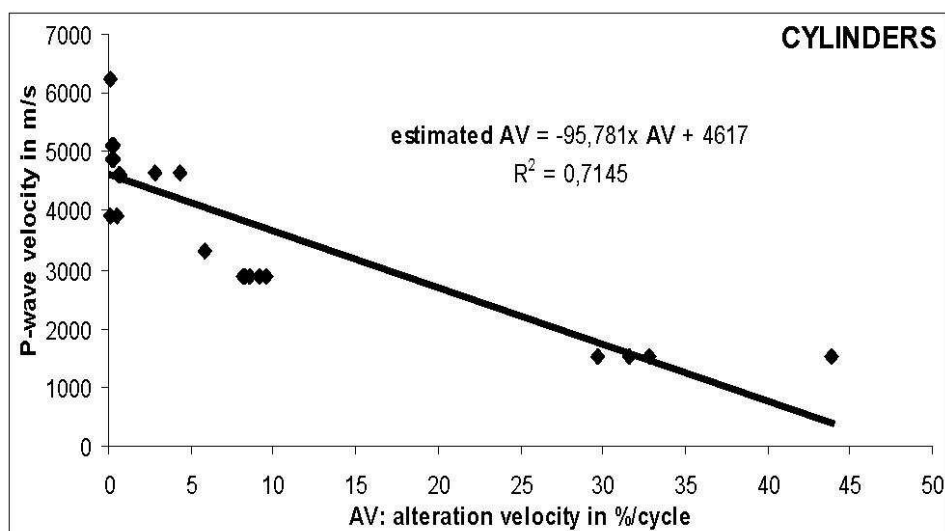


Figure 6b. Estimation of the AV for the second experiment.

Nevertheless, this estimation can be useful because the P-wave velocity is non-destructive and easy to measure on-field, and a mineral analysis can help us to determine if this estimation is relevant or not.

3.3. *Dimension effect*

The resistance of a sample to salt decay has been estimated for both experiments. Now the importance of the dimension of the sample will be discussed.

3.3.1. *Alteration Index*

As shown in 4.2.1., evaporation is a very important phenomenon when it comes to salt crystallization in porous networks (Rodriguez-Navarro and Doehne 1999). When evaporation is impossible through a face of a sample, this face is not altered and the weathering of the whole sample is slowed down (Angeli et al. 2006). The easier the sample can be dried, the easier sodium sulphate can crystallize in the porous network.

For the same volume, the core of a sample will be dried faster if there is a dimension which is significantly smaller than the others. Figure 7 explains this fact in a very simple way. Hence, the smallest dimension of a sample will affect its resistance to salt weathering. It can be considered in multiplying the slope of the linear regression by the smallest dimension of a sample (4cm for the first experiment, 2.5cm for the second) for each experiment. It gives two

values of 0.99 and 1.20 cm, which differ from 18% (the difference between the two slopes is 50%).

It is important to notice that this estimation is only relevant for the middle term behaviour. For the very short term, other parameters are to be taken in account: for instance, the cubes will alter faster than cylinders since there are more edges and corners.

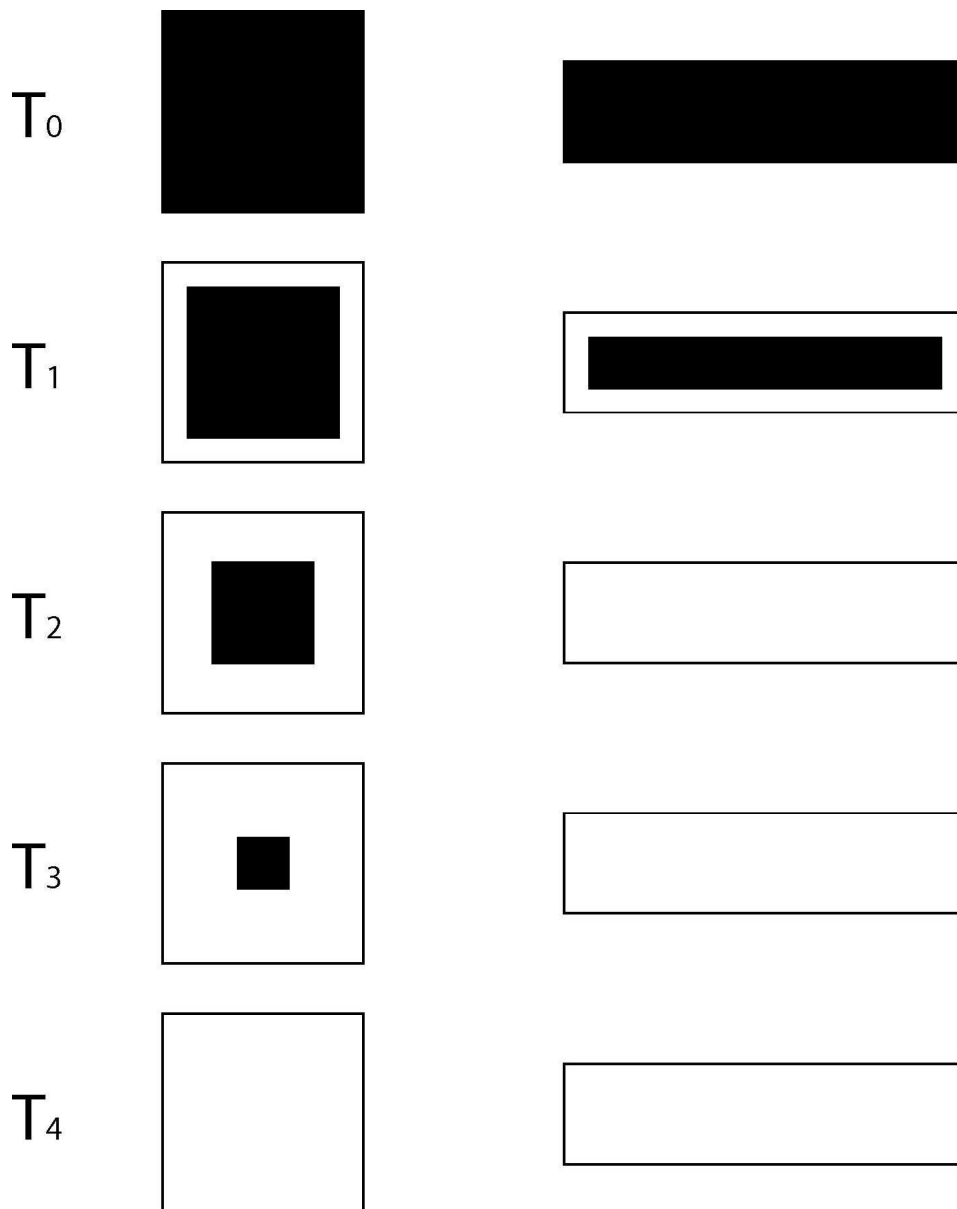


Figure 7. Simplified evaporation kinetics of two samples of the same volume but different dimensions. The same thickness of water evaporates in the two samples between two instants. The part of the sample which is wet is in *black*, the dry part is in *white*.

3.3.2. Alteration Velocity

For a given sample, AV will depend on the total surface exposed to evaporation. The samples seem to lose a small thickness of grain on every side that was exposed to evaporation. During stage III, the samples seem to lose a small thickness of material during each cycle. By using the same approximation technique as in last paragraph, this fact can be estimated by dividing (not multiplying because a resistant stone has a low AV) the slope of the linear regression by the total surface of the sample (the samples are immersed in our experiments). It gives two values of 4.33 and 4.54 cm⁻², which differ from 4.5% (the difference between the two slopes was 66%).

Nevertheless, those two evaluations need more data to be confirmed, with more shapes tested. In addition to that, the linear regressions in both cases are very approximate. Anyway it is clear that the shape and size of a sample has an influence on its alteration. For a given volume, the most resistant shape is the one that minimizes the exposed surface and maximizes the smallest dimension: the sphere.

Conclusion

A new way for evaluating accelerated ageing through crystallization of salt is proposed. It is composed of two parameters: alteration index (AI) and alteration velocity (AV). It is then possible to classify the different stones according to these two indicators: the results show that the stones that are the most resistant at first (high AI) are not necessarily the most resistant at the end (low AV). It allows characterizing the alteration during the whole test and not just at the end of it.

Another classification of alteration is also proposed. It takes into account the alteration patterns: homogeneous, heterogeneous or anisotropic. This can be estimated by a microstructural study of the stone.

The accelerated ageing can be decomposed into 3 stages. Stage I corresponds to the weight gain due to salt crystallization in the pores. Stage II, when it exists, is an intermediate stage during which there is a competition between salt supply and material loss. Stage III corresponds to the long term alteration, when the weight loss is approximately linear.

Two estimators have been given for respectively AI and AV. Those estimators underline the fact that it is crucial to perform a microstructural study of the stone to predict its weathering. The main result is that the P-wave velocity in the stone gives a good idea of the long term behaviour of the stone: the higher the P-wave velocity, the more resistant the stone.

The shape of a sample has also an important influence on its weathering through crystallization of salts, because it directs the evaporation kinetics. A sample that has a significantly smaller dimension with respect to the two others will alter faster as a more regular, the most resistant shape being the sphere.

Acknowledgements

The authors would like to thank M. Pallix from ROCAMAT (Saint-Maximin-sur-Oise) for providing LL, RL and FL, and M. Oliveira (Moigny-sur-Ecole) for the other samples.

References

Angeli M, Bigas JP, Menéndez B, Hébert R, David C (2006) Influence of capillary properties and evaporation on salt weathering of sedimentary rocks. Paper presented at the Heritage Weathering and Conservation conference in Madrid, 21-24 june, 2006

Beck K, Al-Mukhtar M, Rozenbaum O, Rautureau M (2003) Characterization, water transfer properties and deterioration in tuffeau: building material in the Loire valley - France. *Building and Environment* 38:1151-1162

Benavente D, García del Cura MA, García-Guinea J, Sánchez-Moral S, Ordoñez S (2004a) The role of pore structure in salt crystallisation in unsaturated porous stone. *Journal of Crystal Growth* 260:532-544

Benavente D, Garcia del Cura MA, Fort R, Ordoñez S (2004b) Durability of porous building stones from pore structure and strength. *Engineering Geology* 74:113-127

EN 12370 (1999) Natural stone test methods – Determination of resistance to salt crystallization. 1999-03

Flatt RJ (2002) Salt damage in porous materials: how high supersaturations are generated. *Journal of Crystal Growth* 242:435-454

Hammecker (1993) Importance des transferts d'eau dans la dégradation des pierres en œuvre. Ph-D Thesis University of Strasbourg, France

Kracek FC (1928) *Int. Critical Tables* 3 (p. 371)

Rodriguez-Navarro C, Doehne E (1999) Salt weathering: influence of evaporation rate, supersaturation and crystallization pattern. *Earth Surface Processes and Landforms* 24:191-209

Rodriguez-Navarro C, Doehne E, Sebastian E (2000) How does sodium sulphate crystallize? Implications for the decay and testing of building material. *Cement and Concrete Research* 30:1527-1534

Rose DA (1963) Water movement in porous materials – II: the separation of the components of water movement. *British Journal of Applied Physics* 14 :491-496

Scherer G (1999) Crystallization in pores. *Cement and Concrete Research* 29:1347-1358

Scherer G (2004) Stress from crystallization of salt. *Cement and Concrete Research* 34 :1613-1624

Steiger M (2005) Crystal growth in porous materials – I: the crystallization pressure of large crystals. *Journal of Crystal Growth* 282:455-469